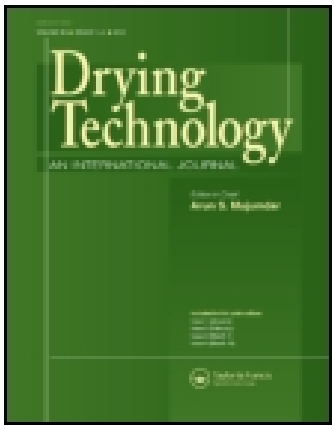

Drying Technology: An International Journal
Publication details, including instructions for authors and subscription information:
http://www.tandfonline.com/loi/ldrt20

Analysis of the Shrinkage Effect on Mass Transfer During Convective Drying of Sawdust/Sludge Mixtures

Jie Li [a], Lyes Bennamoun [b], Laurent Fraikin [a], Thierry Salmon [a], Dominique Toye [a], Raphael Schreinemachers [c] & Angélique Léonard [a]

[a] Laboratory of Chemical Engineering, Department of Applied Chemistry, University of Liège, Liège, Belgium

[b] Department of Mechanical Engineering, Faculty of Engineering, University of New Brunswick, Fredericton, New Brunswick, Canada

[c] Industrie du Bois Vielsalm & Cie SA, Zoning Industriel de Burtonville, Vielsalm, Belgium

Accepted author version posted online: 27 May 2014.Published online: 15 Sep 2014.

To cite this article: Jie Li, Lyes Bennamoun, Laurent Fraikin, Thierry Salmon, Dominique Toye, Raphael Schreinemachers & Angélique Léonard (2014) Analysis of the Shrinkage Effect on Mass Transfer During Convective Drying of Sawdust/Sludge Mixtures, Drying Technology: An International Journal, 32:14, 1706-1717, DOI: 10.1080/07373937.2014.924136

To link to this article: http://dx.doi.org/10.1080/07373937.2014.924136

Drying Technology, 32: 1706–1717, 2014

ISSN: 0737-3937 print/1532-2300 online
DOI: 10.1080/07373937.2014.924136

Taylor & Francis
Taylor & Francis Group

Analysis of the Shrinkage Effect on Mass Transfer During Convective Drying of Sawdust/Sludge Mixtures

Jie Li,[1] Lyes Bennamoun,[2] Laurent Fraikin,[1] Thierry Salmon,[1] Dominique Toye,[1] Raphael Schreinemachers,[3] and Angélique Léonard[1]

[1]*Laboratory of Chemical Engineering, Department of Applied Chemistry, University of Liège, Liège, Belgium*
[2]*Department of Mechanical Engineering, Faculty of Engineering, University of New Brunswick, Fredericton, New Brunswick, Canada*
[3]*Industrie du Bois Vielsalm & Cie SA, Zoning Industriel de Burtonville, Vielsalm, Belgium*

Convective drying of wastewater sludges and sawdust/sludge mixtures was studied. The first part of this work was an experimental study performed in a cross-flow convective dryer using 500 g of wet material extruded through a disk with circular dies of 12 mm. The results showed that the sawdust addition has a positive impact on the drying process from a mass ratio of 2/8, on a dry basis, with observed drying rates higher than the original sludge. The second part of this work consisted of developing a drying model in order to identify the internal diffusion coefficient and convective mass transfer coefficient from the experimental data. A comparison was made between fitted drying curves, well represented by the Newton's model, and the analytical solutions of the diffusion equation applied to a finite cylinder. Variations of dimensional characteristics, such as the volume and exchange surface of the sample bed, were obtained by X-ray tomography. This technique allowed us to confirm that shrinkage, which is an important phenomenon occurring during sludge and sawdust/sludge mixture drying, must be taken into account. The results showed that both the internal diffusion coefficient and convective mass transfer coefficient were affected by mixing and sawdust addition. The internal diffusion coefficient changed from 7.77×10^{-9} m^2/s for the original sludge to 7.01×10^{-9} m^2/s for the mixed sludge and then increased to 8.35×10^{-9} m^2/s for the mixture of a mass ratio of 4/6. The convective mass transfer coefficient changed from 9.70×10^{-8} m/s for the original sludge to 8.67×10^{-8} m/s for the mixed sludge and then increased to 12.09×10^{-8} m/s for the mixture of a mass ratio of 4/6. These results confirmed that sawdust addition was beneficial to the sludge drying process as the mass transfer efficiency between the air and material increased. Reinforcing the texture of sludge by adding sawdust can increase the drying rate and decrease the drying time, and then the heat energy supply will be reduced significantly. The study also showed that neglecting shrinkage phenomenon resulted in an overestimation for the internal diffusion coefficient for the convective drying of sludges and sawdust/sludge mixtures.

Correspondence: Jie Li, Laboratory of Chemical Engineering, Department of Applied Chemistry, University of Liège, Liège, Belgium; E-mail: jie.li@ulg.ac.be

Color versions of one or more of the figures in the article can be found online at www.tandfonline.com/ldrt.

Keywords Diffusion coefficient; Drying kinetics; Mass transfer coefficient; Sawdust; Sewage sludge; X-ray tomography

INTRODUCTION

Due to the increased water demand of the world's population, together with stringent requirements for discharge into the natural environment, the quantity of sludge generated from wastewater treatment plants (WWTPs) is continuously increasing. For example, roughly 9.18 million tons of dry solid sludge is produced in China per year,[1,2] around 5.4 million tons in the United States,[2,3] and more than 11.5 million tons in Europe.[2] Sludge may contain not only organic and inorganic matter, but also bacteria and viruses, oil and grease, nutrients such as nitrogen and phosphorus, heavy metals, and organochlorine compounds.[4] Hence, sludge valorization has become an important issue. Because the sludge still contains more than 95% of water at the outlet of thickeners within wastewater treatment plants, it is necessary to reduce the moisture content. It is difficult to achieve more than 20–30% dry solid contents using classical mechanical dewatering techniques (belt filters, press filters, centrifuges), and thermal drying has become a necessary step before sludge valorization.[5]

However, because of the soft and pasty form of the sludge, thermal drying can be difficult when using technologies requiring an extrusion of feed. Due to the poor stiffness of the sludge, the developed exchange area is rather small, also giving low drying rates. In this work, sawdust addition was proposed as a way of reinforcing the texture of soft and pasty sludge, which is difficult to dry. Reinforcing the texture of sludge can increase the drying rate and decrease the drying time, and then the heat energy supply and operation cost will be reduced significantly. Besides the improvement of drying kinetics, sawdust also brings organic matter, which is useful for further gasification or

combustion processes. Hence, it makes sense for sludges that are difficult to dry because they are pasty. Sawdust is produced in large quantities by the forest industry and also needs safe disposal solutions.[6] Sawdust is normally applied in the manufacture of compressed biofuels or for making compressed wood boards,[7] but new applications should be explored. A mixing machine will be added to the typical industrial sludge drying set-up, which consists of a belt dryer and sludge extruder. Sawdust/sludge mixtures are extruded and then dried in the belt dryer. The investment cost will slightly increase because of the addition of the mixing machine. However, as mentioned earlier, the operation cost will be reduced significantly because of the reduction of the drying time; thus, the overall cost will be reduced.

Both heat and mass transfer problems are complicated during sludge drying due to their complicated structures, but they are necessary and useful for industries. For sawdust/sludge mixtures, the inner structure will be even more complex. In addition, their thermal and physical properties change because of shrinkage. Reyes et al.[8] determined the water diffusion coefficient during wastewater sludge drying by comparing experimental data and an analytical solution of the diffusion equation.[9] However, the problem was simplified by considering an infinite length in opposition to thickness. Font et al.[10] also determined the diffusion coefficient during sewage sludge drying. They added the skin effect, a gradient of moisture inside the particle, in their mathematical formulation represented by correcting factors. Bennamoun et al.[5] introduced the shrinkage effect in mathematical modeling for convective drying of wastewater sludge. A comparison between two calculations, with shrinkage and without shrinkage, showed that neglecting shrinkage leads to an overestimation of the diffusion coefficient by almost a factor of 2. In their work, the volume and surface of the sludge bed were estimated from sludge density, based on the extrusion diameter and initial mass of one extruded particle forming the sludge bed, and making some assumptions about the length of extrudates.

In this context, the present work aims to investigate the shrinkage effect on the internal diffusion coefficient and mass transfer coefficient for convective drying of sewage sludges and sawdust/sludge mixtures. Shrinkage and subsequent crack formation are important phenomena in sludge drying because the sample loses its moisture and exhibits volumetric reduction, and then the internal stresses exceed the tensile strength.[11–15] First, mathematical modeling for determination of diffusion coefficients was established and convective drying experiments of sludges and sawdust/sludge mixtures were done. X-ray tomography, a non-destructive imaging technique, is used to get the volume, surface, and porosity of the sample bed directly. The utilization of X-ray tomography allowed us to follow the changes that take place in the texture,[16–18] cracking,[11,19,20] surface,[21] and volume and shrinkage.[11,20,22] The diffusion coefficients and convective mass transfer coefficients, with and without considering shrinkage, were determined for sludges and sawdust/sludge mixtures using the volume and exchange surface obtained from X-ray tomography. Finally, the mass transfer processes of different samples were compared and the influence of sawdust addition on convective drying of sludges and sawdust/sludge mixtures was analyzed.

MATERIALS AND METHODS

Materials

Sludge was collected after the mechanical dewatering step in one WWTP located near the University of Liège (Grosses Battes, Belgium). The initial moisture content was determined according to standard methods[23] and the value was around 85.5% (wet basis). Before drying, the sludge was stored at a temperature of 4°C to keep drying properties the same during storage.[24] Table 1 gives some physical and chemical characteristics of the sludge used.

Pine sawdust was collected from a wood pellet factory (“Industrie du bois,” Vielsalm, Belgium) and the initial moisture content (wet basis) was around 30%. Table 2 gives the size distribution of the sawdust used.

In this article, the drying behavior of several samples was tested: the original sludge, the mixed sludge (the original sludge after mixing without sawdust), and some mixtures (the original sludge after mixing with sawdust). A kitchen machine (KM1000, PROline) with a beater was used to prepare the mixed sludge and mixtures. The mass ratios (expressed on a dry matter basis for both the sludge and sawdust) of sawdust/sludge were 1/9, 2/8, 3/7, and 4/6. Sludge and sawdust were mixed during 30 s at 40 rpm because longer mixing time and higher mixing velocity will decrease the rigidity of sludge extrudates and the drying rate. The same protocol was used to mix the original

TABLE 1
Characteristics of the sludge used

Product	Sludge origin	Initial moisture content	Volatile solids
Sludge	WWTP of Grosses Battes, Liège, Belgium	5.90 kg/kg of dry matter	63.79% in total solid

TABLE 2
Size distribution of the sawdust used

Diameter	<0.6 mm	0.6–1.7 mm	1.7–5 mm
Mass percent (%)	20.14%	45.03%	34.83%

sludge without any sawdust addition. Samples were then extruded through a disk with circular dies of 12 mm before drying, forming a bed of extrudates on the dryer-perforated grid. The weight of the bed of extrudates was fixed at 500 g in all experiments.

Methods

Pilot-Scale Dryer

The drying experiments were carried out in a discontinuous pilot-scale dryer reproducing most of the operating conditions prevailing in a full-scale continuous belt dryer, as shown in Fig. 1. A fan (a) draws in ambient air and then the air is heated up to the required temperature by a set of electrical resistances (b). If needed, the air is humidified just after heating by adding vapor from a vapor generator. Hot air flows through the bed of sludge extrudates (c), which lies on a perforated grid (d) linked to scales (e). The inner diameter of the sample holder is 160 mm. Three operating parameters may be controlled: air temperature, superficial velocity, and humidity. In this study, the temperature was 80°C, with air velocity fixed at 2 m/s. No additional air humidification was carried out. During the whole study, the ambient air humidity was close to 0.004 $kg_{water}/kg_{dry\ air}$. Drying experiments include continuous experiments and intermittent experiments. For continuous drying experiments, the sample was continuously weighed during the drying test until the weight reached a constant and its mass was recorded every 10 s. For intermittent drying experiments, the sample was taken out several times (7 min, 15 min, 22 min, 30 min, 45 min, 60 min, 90 min, 120 min, and 150 min) in order to perform the X-ray tomography experiments. The mass of each sample inside the dryer was recorded every 10 s as well.

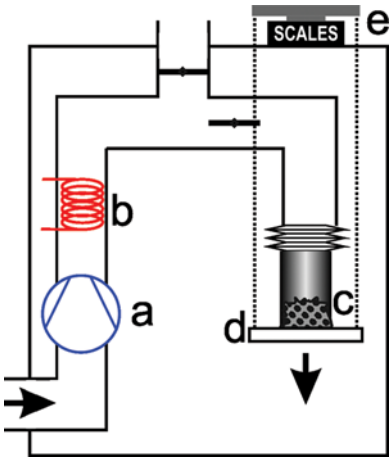

FIG. 1. Pilot-scale dryer.

X-Ray Tomography

X-ray tomography was used to determine the influence of sawdust addition on structures of beds of extrudates. This non-invasive technique, originally developed for medical applications, allows for obtaining 2D cross-sections and 3D images of the bed. The volume, bed porosity, and total exchange surface available for heat and mass transfer were determined by the image analysis of tomographic images.

The X-ray tomographic device used in this paper was a high-energy X-ray tomograph, first presented by Toye et al.[25] The generator is a Baltograph CS450A (Balteau NDT, Belgium), which may be operated between 30 and 420 kV. The X-ray source is an oil-cooled, bipolar TSD420/0 tube (Comet and Balteau NDT), whose intensity may be varied between 2 and 8 mA, depending on the voltage used. A lead collimator produces a 1-mm-thick fan beam. The detector is an X-Scan 0.4f2-512-HE, manufactured by Detection Technology (Finland). This detector consists of a linear array of 1280 photodiodes, each coupled with a CdWO4 scintillator. The mechanical rig, designed by Pro Actis, Belgium, consists of two parts: a source-detector arm and a rotating table on which the object to be scanned is fixed. This arm is embedded in a carriage that slides on two vertical high-precision machined rails. The rig allows vertical movement up to 3780 mm, keeping vertical and horizontal errors within 1 mm. The maximum diameter of the sample that can be tested is 0.45 m.

The extrudates bed to be scanned is put on the turntable, whose rotation is obtained by a synchronous motor equipped with a frequency validator which is supervised by the data acquisition system. Once the sample is put on the turntable, projections of several slices of the bed are recorded around 360°. Reconstruction of cross-sections was obtained by a classical, linear back-projection algorithm adapted to the fan beam geometry implemented in the Fourier domain. The 3D image was obtained by stacking 2D reconstructed cross-sections.

In our experiments, the energy of the source was 420 kV and 3.5 mA, the pixel size of the image was 0.36 mm, and the distance between two slices was 4.4 mm.

Image Analysis

Gray-level images provided by X-ray tomography are formed by two phases: the void at low gray levels (dark pixels) and sludge extrudates at high gray levels (bright pixels). A circular mask, corresponding to the inner diameter of the drying chamber, was first constructed to isolate the sludge

bed from the background. Then binarization (i.e., assigning the value 1 to pixels belonging to the sludge and the value 0 to the pixel belonging to the voids) was performed following Otsu's method.[26]

The object volume was the total volume of binarized objects within the volume-of-interest (VOI) and the calculation method was the number of voxels of binarized solid objects in the VOI times the voxel volume.

The calculation method of the total exchange surface was the total perimeter of the air/solid interface in 2D images (i.e., the pixel edges shared by void and solid pixels) times the distance between two slices.

All of these operations were implemented in Matlab (Matworks), using the image analysis toolbox version 6.0.

Mathematical Model

Empirical Models

At first, the drying curves can be expressed by semi-theoretical and theoretical thin drying models. The models are as follows:

Newton's model[27]

$$X^* = \exp(-k\mathrm{t}) \tag{1}$$

Page's model[28]

$$X^* = \exp(-k\mathrm{t}^n) \tag{2}$$

Henderson and Pabis' model[29]

$$X^* = a\exp(-k\mathrm{t}) \tag{3}$$

Logarithmic's model[30]

$$X^* = a\exp(-k\mathrm{t}) + c \tag{4}$$

Wang and Singh's model[31]

$$X^* = a + b\mathrm{t} + c\mathrm{t}^2 \tag{5}$$

The dimensionless moisture content X^* is given by the following equation:

$$X^* = X/X_0 \tag{6}$$

The illegibility of the models were confirmed by calculating the correlation coefficient (R^2), the reduced chi-square (χ^2), the mean bias error (MBE), and the root mean square error (RMSE). The last three criteria were represented statistically by the following equations:

$$\chi^2 = \frac{\sum_{\mathrm{i}=1}^{\mathrm{N}}\left(X^*_{\mathrm{pre,i}} - X^*_{\mathrm{exp,i}}\right)^2}{\mathrm{N}-\mathrm{p}} \tag{7}$$

$$\mathrm{MBE} = \frac{1}{\mathrm{N}}\sum\nolimits_{\mathrm{i}=1}^{\mathrm{N}}\left(X^*_{\mathrm{pre,i}} - X^*_{\mathrm{exp,i}}\right) \tag{8}$$

$$\mathrm{RMSE} = \left[\frac{1}{\mathrm{N}}\sum_{\mathrm{i}=1}^{\mathrm{N}}\left(X^*_{\mathrm{pre,i}} - X^*_{\mathrm{exp,i}}\right)^2\right]^{\frac{1}{2}} \tag{9}$$

Fick's Second Law

For describing the drying process during the decreasing rate period, the concept of effective moisture diffusivity (D_{eff}) has been accepted as the basic mechanism of the moisture movement inside the drying material.[5,8,9]

According to Fick's second law, the governing equations for transient mass transfer in slab- and cylinder-shaped solid objects are given as follows[9,32]:

Slab (in Cartesian coordinates x, y, z)

$$\frac{\partial^2 X}{\partial x^2} + \frac{\partial^2 X}{\partial y^2} + \frac{\partial^2 X}{\partial z^2} = \frac{1}{D_{eff}}\frac{\partial X}{\partial t} \tag{10}$$

Cylinder (in cylindrical coordinates r, θ, z)

$$\frac{1}{r}\frac{\partial}{\partial r}\left(r\frac{\partial X}{\partial r}\right) + \frac{1}{r^2}\frac{\partial^2 X}{\partial \theta^2} + \frac{\partial^2 X}{\partial z^2} = \frac{1}{D_{eff}}\frac{\partial X}{\partial t} \tag{11}$$

Solutions for Eqs. (10) and (11) in three dimensions for different boundary conditions are complicated and can be found in the literature.[9,32] However, the transient transfer in infinite slabs and cylinders can be approached as a one-dimensional problem leading to the simplification of the complex problem. Then, solutions for an infinite cylinder (as a two-dimensional problem in r and z) and an infinite slab (as a three-dimensional problem in x, y, and z) can be derived.[33] For analytical solutions, the initial condition of uniform temperature/mass distribution and third kind of boundary conditions are used.

The initial condition is:

$$t = 0 : X(y,t) = X_0 \quad \mathrm{y} = L \text{ or } R \tag{12}$$

The boundary conditions are:

$$y = 0 : \frac{\partial X(y,t)}{\partial y} = 0 \tag{13}$$

$$y = L : -D_{eff}\frac{\partial X(y,t)}{\partial y} = h_m(X(y,t) - X_\infty) \tag{14}$$

In our investigation, the experimental moisture content of the sample is obtained as the mean value during drying. The volume mean moisture content of the cylinder and slab can be obtained by integrating the solution of analytical equation in the form of infinite series of dimensionless

moisture distribution within the sample over the whole volume. In addition, the infinite series solutions may normally be approximated by the first term of the series.[5,8,34,35] The final solutions for dimensionless mean moisture contents for infinite cylinder and infinite slab are given as:

For an infinite cylinder

$$X^* = \frac{4}{\lambda_1^2}\frac{J_1^2(\lambda_1)}{\lambda_1^2 J_0^2(\lambda_1) + J_1^2(\lambda_1)} exp\left(-\lambda_1^2 F_o\right) \tag{15}$$

Here, λ_1 is given by:

$$Bi = \lambda_1 \frac{J_1(\lambda_1)}{J_0(\lambda_1)} \tag{16}$$

For an infinite slab

$$X^* = \frac{2sin^2\lambda_1}{\lambda_1(\lambda_1 + sin\lambda_1 cos\lambda_1)} exp\left(-\lambda_1^2 F_o\right) \tag{17}$$

Here, λ_1 is given by:

$$Bi = \lambda_1 \ tan \ \lambda_1 \tag{18}$$

In this study, we suppose that moisture diffusion occurs in two-dimensional isotropic directions (r and z directions).[11,36] It is not possible to use the infinite approach because the radius is near to the height of the product. We adopted an approach called a *superimposition* technique,[33,35,37] which consists of providing the solution as the product of two infinite analytical solutions. Therefore, mathematically, we can write:

$$X^*_{Finite\ cylinder} = X^*_{Infinite\ cylinder} \ X^*_{Infinite\ slab} \tag{19}$$

This equation is a function of the Fourier number (F_o), which is equal to

$$F_o = \frac{D_{eff}\, t}{\delta^2} \tag{20}$$

The parameter δ represents the half-thickness for an infinite slab, radius for an infinite cylinder, characteristic dimension for a finite geometry, which is equal to

$$\delta = \frac{V}{S} \tag{21}$$

A simplified approach can be used to predict the drying kinetics for the falling rate period of drying between initial and mean moisture content at time t. Newton's model is a semi-theoretical equation and it is the most adapted approach to compare the results with those of the diffusion model.

A comparison between Newton's model (Eq. (1)) and analytical solutions (Eq. (19)) allowed calculation of the diffusion coefficient using the following equation, as presented by Tripathy and Kumar[34]:

$$D_{eff} = k\frac{\delta^2}{\lambda_1} \tag{22}$$

The drying constant k is directly obtained from the fitting results of Newton's model and λ_1 is obtained from a comparison between Eq. (1) and Eq. (19).

The convective mass transfer can then easily be deduced using

$$h_m = Bi\frac{D_{eff}}{\delta} \tag{23}$$

It is clear by the mean of the two last equations that the coefficients D_{eff} and h_{m} depend on δ, presented as a function of the product dimensions (Eq. (21)), so a change in this parameter, such as during shrinkage, has a direct influence on calculation of D_{eff} and h_{m}.

As mentioned in the introduction, this study takes shrinkage into account. Its introduction during the modeling steps and calculation of variations in the characteristic dimension (δ) are explained as follows.

Shrinkage is a phenomenon that takes place during drying, especially sludge drying, with an important decrease in the volume and characteristic dimensions. However, shrinkage is neglected in some studies dealing with sludge modeling. Shrinkage is represented as follows:

$$Shrinkage = 1 - \frac{V}{V_0} \tag{24}$$

In this study, shrinkage was considered through calculation of variations in the different physical parameters, such as the volume and exchange surface, during drying. The characteristic dimension (δ), which calculated by volume/surface is expressed as a function of the product's moisture content as follows:

$$\delta = X^*\left(\delta_{wet} - \delta_{dry}\right) + \delta_{dry} \tag{25}$$

RESULTS AND DISCUSSION

Drying Kinetics

The results of drying rate vs. normalized moisture content (X/X_0) related to six different samples (sludges and mixtures) are presented in Fig. 2. The shape of drying rate curves is typical of that described by Léonard et al.[21] and Deng et al.[38] for the convective drying of sludge.

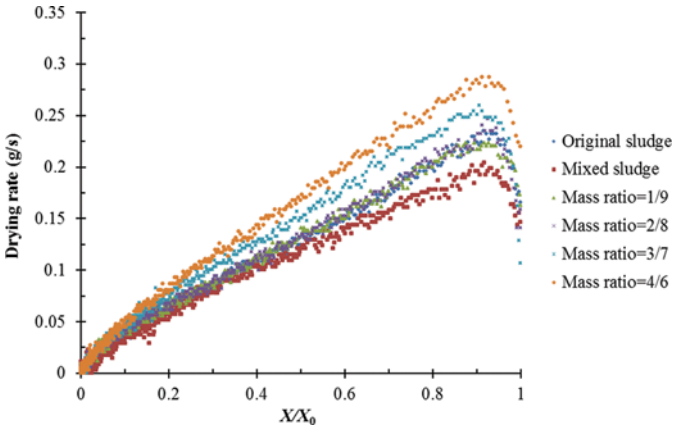

FIG. 2. Drying rate vs. normalized moisture content.

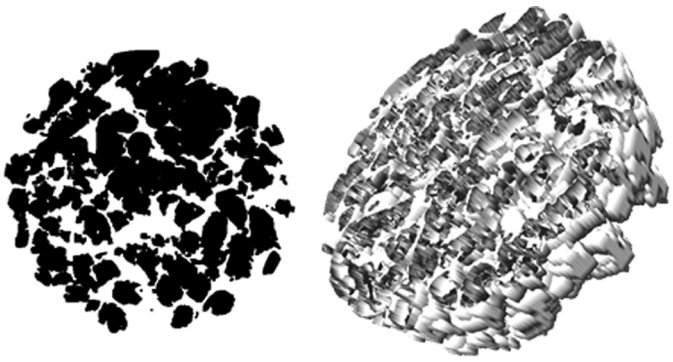

FIG. 3. The 2D cross-section image (a) and 3D image (b) of the original sludge before drying.

As can be seen, the drying rate of the mixed sludge is slower than the original sludge during most of the drying process. Nevertheless, sawdust addition is shown to have a positive impact on the drying process from a mass ratio of 2/8, with observed drying rates in Fig. 2 higher than the original sludge. As explained before,[39] the change of the drying rate is because the total exchange surface decreased after the mixing step but increased with higher sawdust addition.

Figure 3 shows an example of the 2D cross-section image and 3D image of the original sludge before drying. Using image analysis, the volume and total exchange surface can be obtained through X-ray tomographic investigation. The obtained total exchange surface evolution can then be used to estimate the drying flux by dividing the drying rate by the calculated value. Figure 4 shows the results of drying flux vs. X/X_0 related to six different samples. The maximum drying fluxes are almost the same and the values are all between 0.81 and 1.05 $g/(m^2 \cdot s)$. Moreover, the constant drying flux period is very short and the drying falling flux period is dominant.

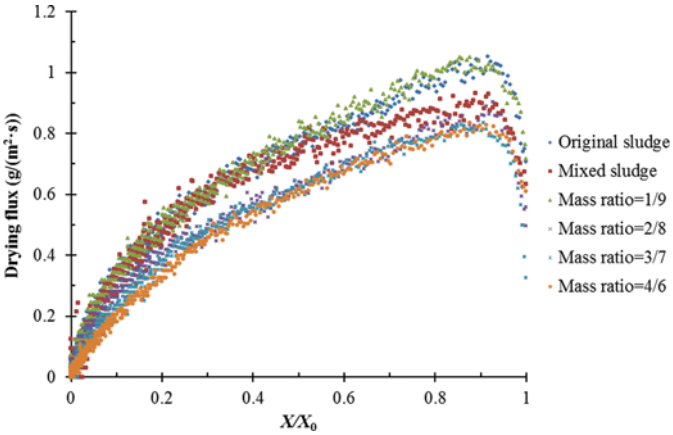

FIG. 4. Drying flux vs. normalized moisture content.

In accordance with the convective drying theory and the results of drying flux, three periods can be identified[5,38]:

- The preheating period exists which represents a period of adaptation of the sample to the drying

TABLE 3
Drying characteristics of sludges and sawdust/sludge mixtures

Sample	Total amount of water (g)	Normalized amount of water	Drying time $95\%_{DS}$ (s)[a]	Average drying rate (g/s)	Normalized drying rate
Original sludge	424	1.000	5370	0.079	1.000
Mixed sludge	426	1.005	7130	0.060	0.759
Mass ratio = 1/9	422	0.995	5970	0.071	0.899
Mass ratio = 2/8	411	0.969	4770	0.086	1.089
Mass ratio = 3/7	407	0.960	4280	0.095	1.203
Mass ratio = 4/6	395	0.932	3720	0.106	1.342

[a]Drying time $95\%_{DS}$: The drying time that the dry solid content (DS) reaches 95%.

TABLE 4
Empirical modeling results for sludges and mixtures

Model	Equation	Sample	Constant	R^2	χ^2	MBE	RMSE
1. Newton	$X^* = \exp(-k\mathrm{t})$	Original sludge	$k = 6.31 \times 10^{-4}$	0.9976	0.0003	−0.0050	0.0164
		Mixed sludge	$k = 5.56 \times 10^{-4}$	0.9977	0.0003	−0.0038	0.0163
		Mass ratio = 1/9	$k = 6.43 \times 10^{-4}$	0.9968	0.0004	−0.0060	0.0200
		Mass ratio = 2/8	$k = 6.64 \times 10^{-4}$	0.9967	0.0004	−0.0059	0.0204
		Mass ratio = 3/7	$k = 7.56 \times 10^{-4}$	0.9969	0.0004	−0.0045	0.0187
		Mass ratio = 4/6	$k = 8.75 \times 10^{-4}$	0.9974	0.0003	−0.0049	0.0176
2. Page	$X^* = \exp(-k\mathrm{t}^n)$	Original sludge	$k = 2.33 \times 10^{-4}$, $n = 1.131$	0.9995	0.0591	−0.2226	0.2430
		Mixed sludge	$k = 1.86 \times 10^{-4}$, $n = 1.142$	0.9999	0.0744	−0.2528	0.2727
		Mass ratio = 1/9	$k = 1.99 \times 10^{-4}$, $n = 1.154$	0.9994	0.0936	−0.2884	0.3058
		Mass ratio = 2/8	$k = 2.03 \times 10^{-4}$, $n = 1.157$	0.9994	0.0964	−0.2931	0.3103
		Mass ratio = 3/7	$k = 2.25 \times 10^{-4}$, $n = 1.163$	0.9997	0.0904	−0.2788	0.3005
		Mass ratio = 4/6	$k = 3.06 \times 10^{-4}$, $n = 1.145$	0.9997	0.0703	−0.2461	0.2650
3. Henderson and Pabis	$X^* = a\exp(-k\mathrm{t})$	Original sludge	$k = 6.60 \times 10^{-4}$, $a = 1.049$	0.9984	0.0002	−0.0055	0.0134
		Mixed sludge	$k = 5.85 \times 10^{-4}$, $a = 1.056$	0.9988	0.0001	−0.0043	0.0120
		Mass ratio = 1/9	$k = 6.77 \times 10^{-4}$, $a = 1.057$	0.9978	0.0003	−0.0067	0.0163
		Mass ratio = 2/8	$k = 7.00 \times 10^{-4}$, $a = 1.059$	0.9978	0.0003	−0.0067	0.0165
		Mass ratio = 3/7	$k = 8.02 \times 10^{-4}$, $a = 1.065$	0.9983	0.0002	−0.0051	0.0141
		Mass ratio = 4/6	$k = 9.21 \times 10^{-4}$, $a = 1.056$	0.9984	0.0002	−0.0055	0.0137
4. Logarithmic	$X^* = a\exp(-k\mathrm{t}) + c$	Original sludge	$k = 6.33 \times 10^{-4}$, $a = 1.051$, $c = -0.012$	0.9990	0.0001	3.47×10^{-10}	0.0107
		Mixed sludge	$k = 5.66 \times 10^{-4}$, $a = 1.058$, $c = -0.009$	0.9991	0.0001	6.20×10^{-11}	0.0103
		Mass ratio = 1/9	$k = 6.41 \times 10^{-4}$, $a = 1.060$, $c = -0.016$	0.9987	0.0002	5.37×10^{-11}	0.0126
		Mass ratio = 2/8	$k = 6.62 \times 10^{-4}$, $a = 1.062$, $c = -0.016$	0.9987	0.0003	-3.96×10^{-11}	0.0129
		Mass ratio = 3/7	$k = 7.74 \times 10^{-4}$, $a = 1.067$, $c = -0.012$	0.9987	0.0001	1.30×10^{-11}	0.0122
		Mass ratio = 4/6	$k = 8.82 \times 10^{-4}$, $a = 1.058$, $c = -0.013$	0.9990	0.0001	2.87×10^{-11}	0.0109
5. Wang and Singh	$X^* = a + b\mathrm{t} + c\mathrm{t}^2$	Original sludge	$a = -3.12 \times 10^{-4}$, $b = 2.19 \times 10^{-8}$	0.9001	0.0109	−0.0264	0.1043
		Mixed sludge	$a = -2.79 \times 10^{-4}$, $b = 1.76 \times 10^{-8}$	0.9048	0.0106	−0.0254	0.1028
		Mass ratio = 1/9	$a = -3.41 \times 10^{-4}$, $b = 2.64 \times 10^{-8}$	0.9336	0.0080	−0.0219	0.0892
		Mass ratio = 2/8	$a = -3.54 \times 10^{-4}$, $b = 2.86 \times 10^{-8}$	0.9361	0.0077	−0.0215	0.0879
		Mass ratio = 3/7	$a = -3.65 \times 10^{-4}$, $b = 2.98 \times 10^{-8}$	0.8885	0.0121	−0.0273	0.1097
		Mass ratio = 4/6	$a = -4.50 \times 10^{-4}$, $b = 4.58 \times 10^{-8}$	0.9188	0.0094	−0.0239	0.0967

conditions. During this period, the drying rate increased considerably.

- The next period observed is the constant drying flux period. This period is very short in the experiments. During this constant rate period, the evaporation takes place at the surface of the wet solid, and the solid assumes a constant equilibrium temperature, just as a free liquid surface is maintained at the wet-bulb temperature of the air.[40] As explained by Deng et al.,[38] the evaporated water in this period is free water.
- The last period has a long falling drying flux, which can be divided into two parts, following Deng et al.[38]; the water removed in the first part is interstitial water and in the second part is surface water.

In order to compare the drying kinetics of different samples, some drying characteristics, including the total amount of evaporated water, normalized amount of water, drying time, average drying rate, and normalized drying rate, are shown in Table 3. The drying time increases and the average drying rate decreases after the sludge is mixed. With a higher sawdust addition, the total amount of water and drying time decrease, but the average drying rate increases. The positive effect of sawdust addition is clearly observed: the drying rate generally increases with increasing the addition of sawdust, while the initial water content decreases as well as the total amount of water to be removed. Indeed, the same mass is introduced for each experiment.

For describing the drying kinetics of sludges and sawdust/sludge mixtures, some drying models were used to fit the drying curves. As mentioned earlier, the falling drying rate period dominates the drying process. These drying models are usually represented by the equation in terms of drying parameters to characterize the changes of mean moisture content during drying. The typical semi-theoretical and theoretical drying models are shown in Eqs. (1)–(5), and Curve Expert software 2.0 was used to achieve the curve fitting.

Table 4 presents selected results obtained for the models. Except for the Wang and Singh's model, the fitting results are all good. The correlation coefficients (R^2) are all high and near 1 and the reduced chi-squares (χ^2), mean bias errors (MBE), and root mean square errors (RMSE) are all small. It also can be observed that the Page's model has the highest value of R^2 and the Logarithmic's model has the lowest values of χ^2, MBE, and RMSE.

Shrinkage

Neglecting the shrinkage effect will bring errors in the determination of mass transfer coefficients. In order to get the evolution of both the volume and surface with the moisture content, intermittent drying experiments were done. To do so, the sample was taken out several times during the course of drying and submitted to X-ray tomography investigation. Figure 5 shows the results of volume shrinkage vs. X/X_0 obtained by using this method. The volumes of sludge decrease nearly linearly with the decreased normalized moisture content for the original sludge and mixed sludge. During the main part of the drying process for the mixtures, the volumes of sawdust/sludge decrease linearly with the normalized moisture content, and then reach a constant value. For sludges, the final volume is nearly 20% of the initial volume and it is in agreement with the results of Léonard et al.[18,41] For sawdust/sludge mixtures, the final shrinkage measured at the end of the drying process becomes smaller with increasing the sawdust, but it remains important. This shrinkage reduction is due to the sawdust that braces the structure of the sample during drying. For example, the final volume is around 50% of the initial volume when the mass ratio of sawdust/sludge is 4/6. Hence, for the analysis of the mass transfer coefficient of sawdust/sludge mixtures, shrinkage cannot be ignored.

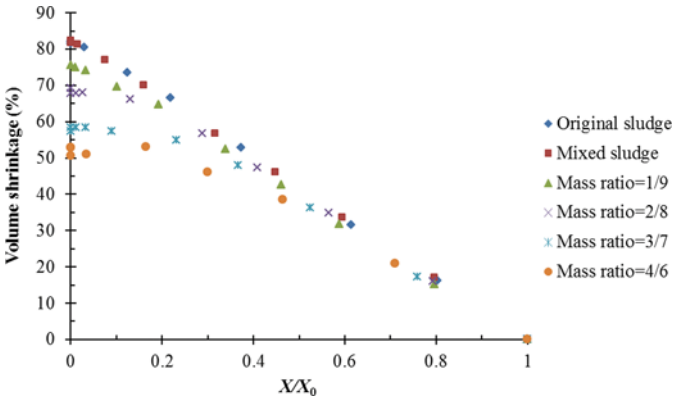

FIG. 5. Bed volume vs. normalized moisture content.

Using the same data, the volume/surface δ vs. X/X_0 was obtained and the results are shown in Fig. 6. The values of

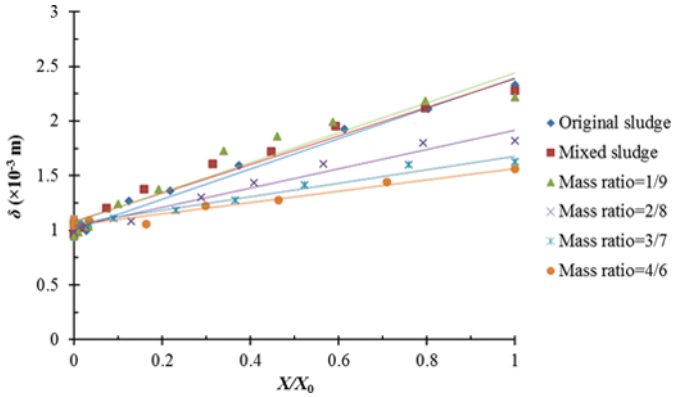

FIG. 6. Volume/surface (δ) vs. normalized moisture content.

TABLE 5
Linear coefficients and equations of the volume/surface

Sample	R^2	Equation
Original sludge	0.9844	$y = 0.00139x + 0.00101$
Mixed sludge	0.9688	$y = 0.00131x + 0.00108$
Mass ratio = 1/9	0.9289	$y = 0.00137x + 0.00107$
Mass ratio = 2/8	0.9692	$y = 0.00089x + 0.00103$
Mass ratio = 3/7	0.9740	$y = 0.00062x + 0.00106$
Mass ratio = 4/6	0.9637	$y = 0.00052x + 0.00105$

the volume/surface decrease nearly linearly with X/X_0 for all sludges and sawdust/sludge mixtures. The linear least-square method is used for the straight line fitting and the results of linear coefficients and equations are shown in Table 5. In fact, for the mixtures, especially with higher sawdust addition, there is a plateau near X/X_0 of zero. There are small errors, but the linear relationship can be accepted because the linear coefficients R^2 are all high. The volume/surface can be treated as decreasing linearly with X/X_0 during drying for each sample in our experiments, and this linear relationship confirmed the correctness of the calculation of the characteristic dimension δ in Eq. (25).

Moreover, the volume/surface δ is clearly lower from a sawdust addition ratio of 2/8, especially at the beginning of drying. The decrease of the volume/surface δ can be related to an enhancement of the surface area available for heat and mass transfer. From the results of the X-ray tomography, we found the volume and surface both increase with increased sawdust addition, but the surface increases more significantly than the volume.[39] However, the difference becomes smaller for increased drying times. At the end of drying, the values of the volume/surface δ are near 0.001 m. It is worth mentioning that the value of the volume/surface after drying increases slightly from adding sawdust. For example, for the original sludge the value is 0.00093 m, and for the mixture of a mass ratio of 4/6 the value is 0.00104 m.

Determination of the Diffusion Coefficient Through Modeling of the Drying Kinetics

Figure 7 shows the variation in the internal diffusion coefficient with X/X_0 after introducing shrinkage in our modeling and simulation work. In each case, the diffusion coefficient decreases while the drying time increases. This dependency with the moisture content is well-known.[42] The results show that the diffusion coefficient of the original sludge is higher than for the mixtures at the beginning of drying and then becomes smaller during the course of drying. For the mixtures, the decrease of the diffusion coefficient rate is smaller for the high ratio of added sawdust.

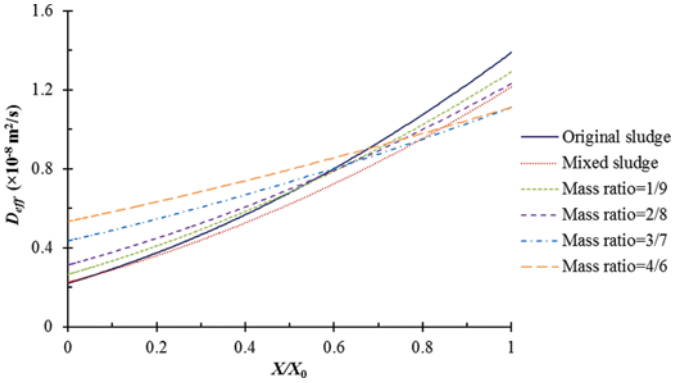

FIG. 7. Variation in the internal diffusion coefficient with the normalized moisture content.

Below the moisture content of 0.6, the trend is clear: the diffusion coefficients of sawdust/sludge mixtures increase with the added amount of sawdust. Moreover, the results show that the mixing step has a clear negative impact on the diffusion coefficient throughout the drying process.

In fact, the diffusion coefficient depends on the internal moisture content and compactness of the sample. When the internal moisture content increases or the sample bed becomes more compact, the diffusion coefficient increases. The moisture contents of the original sludge and mixed sludge are almost the same, but the mixed sludge becomes more compact, so the diffusion coefficient decreases. With more sawdust, the sample bed becomes less compact but the moisture content decreases. During the drying process, for all samples, the moisture content decreases and the sample bed becomes more compact because of the shrinkage effect. Moreover, the sample bed is less compact with increasing addition of sawdust. According to the results in Fig. 7, the change of moisture content of a sample dominates in the beginning of drying, but then the compactness of the sample gradually plays an important role during drying.

$D_{eff,avr}$ is the average diffusion coefficient during the whole drying process and is calculated as follows:

$$D_{eff,\,avr} = \frac{\int_{X_{initial}}^{X_{final}} D_{eff}(X)dX}{\int_{X_{initial}}^{X_{final}} dX} \tag{26}$$

A comparison of results of diffusion coefficients obtained with or without consideration of the shrinkage effect is presented in Table 6. The diffusion coefficient changed from 7.77×10^{-9} m^2/s for the original sludge to 7.01×10^{-9} m^2/s for the mixed sludge and then increased to 8.35×10^{-9} m^2/s for the mixture of a mass ratio of 4/6. These results are within the normally expected range of D_{eff} (10^{-11} to 10^{-9} m^2/s)[43] and they are similar to those results obtained in the case of sludge by Bennamoun et al.[5]

TABLE 6
Influence of sawdust addition on the diffusion coefficient

Sample	$D_{eff,avr}(\times 10^{-9}\,m^2/s)$ with shrinkage	$D_{eff,avr}(\times 10^{-9}\,m^2/s)$ without shrinkage
Original sludge	7.77	13.89
Mixed sludge	7.01	12.15
Mass ratio = 1/9	7.71	12.91
Mass ratio = 2/8	7.73	12.31
Mass ratio = 3/7	7.85	11.10
Mass ratio = 4/6	8.35	11.12

and Reyes et al.,[8] for mushrooms by Xanthopoulos et al.,[44] for potatoes by Ruiz-López et al.,[45] and for beads by Ambrożek et al.[46]

As can be seen, the comparison presented in Table 6 confirmed that neglecting the shrinkage effect can produce erroneous results. This is reflected in two aspects: first, because the diffusion coefficient calculated without consideration of shrinkage was bigger than the value obtained when shrinkage was considered. Second, the diffusion coefficient obtained with consideration of shrinkage increases with increasing the addition of sawdust while it decreases without consideration of shrinkage.

Determination of the Mass Transfer Coefficient

The Biot number B_i can be obtained by the analytical solution proposed by Eqs. (15)–(18). Moreover, the volume/surface δ and diffusion coefficient D_{eff} were obtained. Thus, the convective mass transfer coefficient can be determined by using Eq. (23). The variation in the mass transfer coefficient with normalized moisture content of different samples is shown in Fig. 8. As can be seen, the convective mass transfer coefficient for the mixed sludge is smaller than for the original sludge. Moreover, the convective mass transfer coefficient increases with increasing the addition of sawdust during the whole drying process.

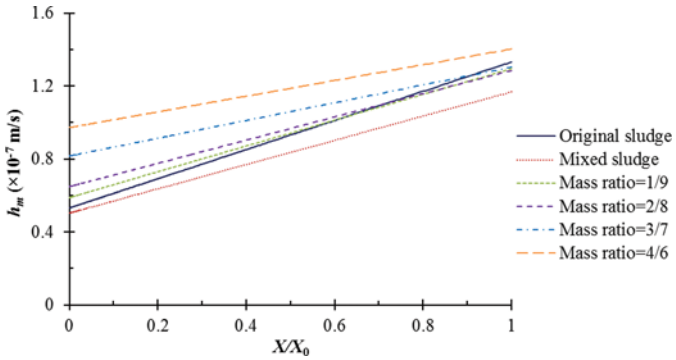

FIG. 8. Variation in the convective mass transfer coefficient with the normalized moisture content.

TABLE 7
Influence of sawdust addition on the convective mass transfer coefficient

Sample	$h_{m,avr}(\times 10^{-8}\,m/s)$ with shrinkage	$h_{m,avr}(\times 10^{-8}\,m/s)$ without shrinkage
Original sludge	9.70	13.31
Mixed sludge	8.67	11.68
Mass ratio = 1/9	9.81	12.95
Mass ratio = 2/8	10.03	12.85
Mass ratio = 3/7	10.87	13.03
Mass ratio = 4/6	12.09	14.02

The average convective mass transfer coefficient $h_{m,avr}$ during the whole drying process is calculated as follows:

$$h_{m,\,avr} = \frac{\int_{X_{initial}}^{X_{final}} h_m(X)dX}{\int_{X_{initial}}^{X_{final}} dX} \tag{27}$$

A comparison of results of mass transfer coefficients obtained with or without consideration of the shrinkage effect is presented in Table 7. These results are similar to those results obtained by Bennamoun et al.[5] and Rahman and Kumar.[37] Moreover, the convective mass transfer coefficient changed from $9.70 \times 10^{-8}\,m/s$ for the original sludge to $8.67 \times 10^{-8}\,m/s$ for the mixed sludge and then increased to $12.09 \times 10^{-8}\,m/s$ for the mixture of a mass ratio of 4/6.

As can be seen, the comparison presented in Table 7 confirmed that calculating the mass transfer coefficient without considering shrinkage can lead to erroneous results, where the value of the coefficient without consideration of shrinkage is bigger than the value obtained when shrinkage was considered. The average mass transfer coefficient increased with the increased sawdust addition, which confirmed that sawdust addition is beneficial to the sludge drying process and the mass transfer efficiency between the air and material increases.

CONCLUSIONS

The developed model allows determination of the internal diffusion coefficient and convective mass transfer coefficient of shrinking bodies is presented. Analytical

solutions of the diffusion equation represented by Fick's second law were applied for a finite cylinder. Moreover, shrinkage was introduced and the parameter δ was calculated by different object volumes and exchange surfaces obtained by X-ray tomography. The value of the volume/surface decreased linearly with decreasing of the normalized moisture content for sludges and sawdust/sludge mixtures.

The drying experiments of sludges and sawdust/sludge mixtures were performed. The drying rate of the mixed sludge was slower than the original sludge. Nevertheless, the sawdust addition showed a positive impact on the drying process from the mass ratio of 2/8, as the observed drying rate was higher than the original sludge. The change of the drying rate is because the total exchange surface decreased after the mixing step but increased with increasing the addition of sawdust.

Semi-theoretical and theoretical drying models, including Newton's model, Page's model, Henderson and Pabis' model, Logarithmic's model, and Wang and Singh's model, were used to fit the drying curves. Except for the Wang and Singh's model, the fitting results were all good. The correlation coefficients (R^2) were all high and near 1 and the reduced chi-squares (χ^2), mean bias errors (MBE), and root mean square errors (RMSE) were all small. Newton's model was the most-adapted approach to compare the results with those of the diffusion model. Accordingly, it was used for modeling in this paper. The drying constants k, the parameter δ, and other parameters related to the model were determined to calculate the internal diffusion coefficient and mass transfer coefficient. The results showed that these two coefficients increased with increasing the addition of sawdust. These results confirmed that adding sawdust is beneficial to the sludge drying process as the diffusion coefficient and mass transfer coefficient increased with increasing the addition of sawdust. Moreover, a comparison between two calculations, with and without considering shrinkage, showed that neglecting the shrinkage effect leads to an overestimation for the two coefficients for convective drying of sludges and sawdust/sludge mixtures.

Further studies can focus on the characterization of the pore texture of the dried sample in relation to the drying and further pyrolysis tests made using thermogravimetric analysis. The impact of sludge origin, including different types of applied treatment, can also be investigated.

NOMENCLATURE

a, b, c, n	Fitting parameters of drying curves
B_i	Biot number
D_{eff}	Effective moisture diffusivity ($m^2 \cdot s^{-1}$)
DS	Dry solid content
F_o	Fourier number
h_m	Convective mass transfer coefficient ($m \cdot s^{-1}$)
J	Bessel function
J_0	Zero-order Bessel function
J_1	First-order Bessel function
k	Drying constant (s^{-1})
L	Half-height of the sample (m)
MBE	Mean bias error
Q	Heat flux ($J \cdot m^{-2} \cdot s^{-1}$)
R	Radius of the sample (m)
R^2	Correlation coefficient
RMSE	Root mean square error
r, θ, z	Cylindrical coordinates
S	Surface (m^2)
t	Time (s)
V	Volume (m^3)
X	Moisture content in dry basis ($kg \cdot kg^{-1}$)
X^*	Dimensionless moisture content
$X^*_{pre,i}$	Predicted moisture ratio
$X^*_{exp,i}$	Experimental moisture ratio
x, y, z	Cartesian coordinates

Greek Letters

χ^2	Reduced chi-square
λ_1	Roots given by Eq. (6) or Eq. (8)
δ	Characteristic dimension (m)

Subscript

0	Initial value
∞	Surrounding
avr	Average
dry	Dry matter
final	Final value of the moisture
initial	Initial value of the moisture
wet	Wet matter

FUNDING

J. Li is grateful to the University of Liège for a postdoctoral grant. L. Bennamoun and L. Fraikin are thankful to the FRS-FNRS for their postdoctoral fellow positions (FRFC projects 2.4596.10 and 2.4596.12).

REFERENCES

1. Deng, W.Y.; Yan, J.H.; Li, X.D.; Wang, F.; Lu, S.Y.; Chi, Y.; Cen, K.F. Measurement and simulation of the contact drying of sewage sludge in a Nara-type paddle dryer. *Chemical Engineering Science* **2009**, *64*(24), 5117–5124.
2. Bennamoun, L. Solar drying of wastewater sludge: A review. *Renewable and Sustainable Energy Reviews* **2012**, *16*(1), 1061–1073.
3. Chen, G.; Yue, P.L.; Mujumdar, A.S. Sludge dewatering and drying. *Drying Technology* **2002**, *20*(4–5), 883–916.
4. Werther, J.; Ogada, T. Sewage sludge combustion. *Progress in Energy and Combustion Science* **1999**, *25*(1), 55–116.
5. Bennamoun, L.; Crine, M.; Léonard, A. Convective drying of wastewater sludge: Introduction of shrinkage effect in mathematical modeling. *Drying Technology* **2013**, *31*(1), 643–654.
6. Berghel, J.; Renstrom, R. Basic design criteria and corresponding results performance of a pilot-scale fluidized superheated atmospheric condition steam dryer. *Biomass and Bioenergy* **2002**, *23*(2), 103–112.

7. Srinivasakannan, C.; Balasubramaniam, N. Drying of rubber wood sawdust using tray dryer. *Particulate Science and Technology* **2006**, *24*(4), 427–439.
8. Reyes, A.; Eckholt, M.; Troncoso, F.; Efremov, G. Drying kinetics of sludge from a wastewater treatment plant. *Drying Technology* **2004**, *22*(9), 2135–2150.
9. Crank, J. *The Mathematics of Diffusion*, 2nd Ed; Clarendon Press: Oxford, UK, 1975.
10. Font, R.; Gomez-Rico, M.F.; Fullana, A. Skin effect in the heat and mass transfer model for sewage sludge drying. *Separation and Purification Technology* **2011**, *77*(1), 146–161.
11. Léonard, A.; Blacher, S.; Marchot, P.; Pirard, J.P.; Crine, M. Measurement of shrinkage and cracks associated to convective drying of soft materials by X-ray microtomography. *Drying Technology* **2004**, *22*(5), 1695–1708.
12. Uday, K.V.; Singh, D.N. Application of laser microscopy for studying crack characteristics of fine-grained soils. *Geotechnical Testing Journal* **2013**, *36*(1), 146–154.
13. Kannan, I.R.; Jayanth, S.; Gurnani, S.; Singh, D.N. Influence of initial water content and specimen thickness on the SWCC of fine-grained soils. *International Journal of Geomechanics* **2013**, *13*(6), 894–899.
14. Uday, K.V.; Singh, D.N. Investigations on cracking characteristics of fine-grained soils under varied environmental conditions. *Drying Technology* **2013**, *31*(11), 1255–1266.
15. Uday, K.V.; Singh, D.N. A generalized relationship for determination of tensile strength of fine-grained soils from shrinkage characteristics. *Drying Technology* **2014**, *32*(7), 869–876.
16. Léonard, A. Study of convective drying of wastewater sludges—Texture follow-up by X-ray microtomography. *Drying Technology* **2004**, *22*(1–2), 417–419.
17. Léonard, A.; Blacher, S.; Pirard, R.; Marchot, P.; Pirard, J.P.; Crine, M. Multiscale texture characterization of wastewater sludges dried in a convective rig. *Drying Technology* **2003**, *21*(8), 1507–1526.
18. Léonard, A.; Blacher, S.; Marchot, P.; Crine, M. Use of the X-ray microtomography to follow the convective heat drying of wastewater sludges. *Drying Technology* **2002**, *20*(4–5), 1053–1069.
19. Hsu, J.P.; Tao, T.; Su, A.; Mujumdar, A.S.; Lee, D.J. Model for sludge cake drying accounting for developing cracks. *Drying Technology* **2010**, *28*(7), 922–926.
20. Tao, T.; Peng, X.F.; Lee, D.J. Thermal drying of wastewater sludge: Change in drying area owing to volume shrinkage and crack development. *Drying Technology* **2005**, *23*(4), 669–682.
21. Léonard, A.; Meneses, E.; Le Trong, E.; Salmon, T.; Marchot, P.; Toye, D.; Crine, M. Influence of back mixing on the convective drying of residual sludges in a fixed bed. *Water Research* **2008**, *42*(10–11), 2671–2677.
22. Ayol, A.; Muslu, D. Response surface methodological approach for the assessment of thermal drying of dewatered municipal sludge. *Drying Technology* **2012**, *30*(14), 1621–1629.
23. ASAE. ASAE Standard no. D245.5; American Society of Agricultural Engineers: St. Joseph, MI, USA, 1996; 452–464.
24. Fraikin, L.; Herbreteau, B.; Chaucherie, X.; Nicol, F.; Crine, M.; Léonard, A. Impact of storage at 4°C on the study of sludge drying emissions. In *2nd European Conference on Sludge Management*, 9–10 September 2010, Budapest, Hungary.
25. Toye, D.; Crine, M.; Marchot, P. Imaging of liquid distribution in reactive distillation packings with a new high-energy X-ray tomograph. *Measurement Science and Technology* **2005**, *16*(11), 2213–2220.
26. Otsu, N. A threshold selection method from gray-level histograms. *IEEE Transactions on Systems, Man, and Cybernetics* **1979**, *9*(1), 62–67.
27. Panchariya, P.C.; Popovic, D.; Sharma, A.L. Thin-layer modelling of black tea drying process. *Journal of Food Engineering* **2002**, *52*(4), 349–357.
28. Basunia, M.A.; Abe, T. Thin-layer solar drying characteristics of rough rice under natural convection. *Journal of Food Engineering* **2001**, *47*(4), 295–301.
29. Pal, U.S.; Chakraverty, A. Thin layer convection-drying of mushrooms. *Energy Conversion and Management* **1997**, *38*(2), 107–113.
30. Midilli, A.; Kucuk, H. Mathematical modeling of thin layer drying of pistachio by using solar energy. *Energy Conversion and Management* **2003**, *44*(7), 1111–1122.
31. Akpinar, E.; Midilli, A.; Bicer, Y. Single layer drying behavior of potato slices in a convective cyclone dryer and mathematical modeling. *Energy Conversion and Management* **2003**, *44*(10), 1689–1705.
32. Carslaw, H.S.; Jaeger, J.C. *Conduction of Heat in Solids*; Clarendon Press: Oxford, UK, 1986.
33. Turhan, M.; Erdoğdu, F. Error associated with assuming a finite regular geometry as an infinite one for modeling of transient heat and mass transfer processes. *Journal of Food Engineering* **2003**, *59*(2–3), 291–296.
34. Tripathy, P.P.; Kumar, S. A methodology for determination of temperature dependent mass transfer coefficient from drying kinetics: Application to solar drying. *Journal of Food Engineering* **2009**, *90*(2), 212–218.
35. Rahman, N.; Kumar, S. Evaluation of moisture diffusion coefficient of cylindrical bodies considering shrinkage during natural convection drying. *International Journal of Food Engineering* **2011**, *7*(1), Art.4.
36. Léonard, A.; Blacher, S.; Marchot, P.; Pirard, J.P.; Crine, M. Image analysis of X-ray microtomograms of soft materials during convective drying. *Journal of Microscopy* **2003**, *212*(2), 197–204.
37. Rahman, N.; Kumar, S. Thermal analysis of natural convective air drying of shrinking bodies. *International Journal of Energy Research* **2007**, *31*(2), 204–217.
38. Deng, W.; Li, X.; Yan, J.; Wang, F.; Chi, Y.; Cen, K. Moisture distribution in sludges based on different testing methods. *Journal of Environmental Sciences* **2011**, *23*(5), 875–880.
39. Li, J.; Fraikin, L.; Salmon, T.; Bennamoun, L.; Toye, D.; Léonard, A. Convective drying of mixtures of sewage sludge and sawdust in a fixed bed. In *4th European Drying Conference*, 2–4 October 2013, Paris, France.
40. Sherwood, T.K. The drying of solids – II. *Industrial and Engineering Chemistry* **1929**, *21*(10), 976–980.
41. Léonard, A.; Blacher, S.; Marchot, P.; Pirard, J.P.; Crine, M. Moisture profiles determination during convective drying using X-ray microtomography. *The Canadian Journal of Chemical Engineering* **2005**, *83*(1), 127–131.
42. Zogzas, N.P.; Maroulis, Z.B. Effective moisture diffusivity estimation from drying data: A comparison between various methods of analysis. *Drying Technology* **1996**, *14*(7–8), 1543–1573.
43. Usub, T.; Lertsatitthankorn, C.; Poomsa-ad, N.; Wiset, L.; Siriamornpun, S.; Soponronnarit, S. Thin layer solar drying characteristics of silkworm pupae. *Food and Bioproducts Processing* **2010**, *88*(2–3), 149–160.
44. Xanthopoulos, G.; Nastas, C.V.; Boudouvis, A.G.; Aravantinos-Karlatos, E. Color and mass transfer, kinetics during air drying of pretreated oyster mushrooms (Pleurotus ostreatus spp.). *Drying Technology* **2014**, *32*(1), 77–88.
45. Ruiz-López, I.I.; Ruiz-Espinosa, H.; Pacheco-Aguirre, F.M.; García-Alvarado, M.A. Drying of food products shaped as longitudinal sections of solid and annular cylinders: Modeling and simulation. *Drying Technology* **2013**, *31*(10), 1148–1159.
46. Ambrożek, B.; Nastaj, J.; Gabruś, E. Modeling and experimental studies of adsorptive dewatering of selected aliphatic alcohols in temperature swing adsorption system. *Drying Technology* **2013**, *31*(15), 1780–1789.